

## Injury and recovery of pyramidal neurons in the rat hippocampus after a single episode of oxidative stress induced by intracerebroventricular injection of ferrous ammonium citrate

Wei-Yi ONG<sup>a\*</sup>, Su-Fung LING<sup>b</sup>, Jin-Fei YEO<sup>b</sup>, Chuang-Chin CHIUEH<sup>c</sup>,  
Akhlq A. FAROOQUI<sup>d</sup>

<sup>a</sup> Department of Anatomy, National University of Singapore, Lower Kent Ridge Road, Singapore 119260, Singapore

<sup>b</sup> Department of Oral and Maxillofacial Surgery, National University of Singapore, Lower Kent Ridge Road, Singapore 119260, Singapore

<sup>c</sup> College of Pharmacy, Taipei Medical University, Taipei City 110, Taiwan (ROC)

<sup>d</sup> Department of Molecular and Cellular Biochemistry, The Ohio State University, Columbus, Ohio 43210, USA

(Received 7 December 2004; accepted 25 May 2005)

**Abstract** – The present study was carried out to elucidate the effect of a single episode of oxidative stress on pyramidal neurons of the rat hippocampus. A significant increase in the number of neurons that were immunolabeled for the toxic lipid peroxidation product, 4-hydroxynonenal (HNE) was observed in field CA3 of the hippocampus, at 1 day, 7 days and 14 days after intracerebroventricular injection of 1  $\mu$ L of 5mM ferrous ammonium citrate, compared to ammonium citrate injected controls at these time points. The number of HNE positive cells was fewer at 14 days, compared to 1 day, after ferrous ammonium citrate injection. The changes in HNE immunoreactivity were paralleled by changes in cytoplasmic phospholipase A<sub>2</sub> (cPLA<sub>2</sub>) labeling in the pyramidal neurons in adjacent sections, suggesting that some of the HNE could have arisen as a result of peroxidation of arachidonic acid that was released by cPLA<sub>2</sub>. Interestingly, despite the HNE and cPLA<sub>2</sub> labeling, no loss of neurons was observed in adjacent Nissl and Fluoro-Jade stained sections. Electron microscopy also showed that the HNE or cPLA<sub>2</sub> labeled cells had features of injured neurons, rather than necrotic neurons. The reduction of HNE immunoreactivity in neurons at 14 days after oxidative injury, and the absence of cell loss at any of the time intervals, shows that hippocampal pyramidal neurons have remarkable ability to recover from a single episode of oxidative stress, if repeated injury such as seizures / excitotoxicity could be avoided.

**iron / neurodegeneration / 4-hydroxynonenal / cytosolic phospholipase A<sub>2</sub> / lipid peroxidation / antioxidant defenses**

**Abbreviations:** AP-1: activator protein-1; CA: cornu ammonis; cPLA<sub>2</sub>: cytosolic phospholipase A<sub>2</sub>; DAB: 3,3'-diaminobenzidine tetrahydrochloride; HNE: 4-hydroxynonenal; NF- $\kappa$ B: nuclear factor-kappa B; N-TBS: nickle-tris-buffered saline; PBS: phosphate-buffered saline; PUFA: polyunsaturated fatty acids; ROS: reactive oxygen species.

\* Corresponding author: antongwy@nus.edu.sg

## 1. INTRODUCTION

Cellular redox is maintained by a balance between the production of reactive oxygen species (ROS) and their destruction by the cellular antioxidant systems [1]. Brain tissue is particularly vulnerable to oxidative stress not only due to its high oxidative metabolism and high concentrations of polyunsaturated fatty acids (PUFA), but also due to low levels of catalase and glutathione, and limited amounts of superoxide dismutase and chemical oxidants [2].

In neural membrane phospholipids, PUFA, particularly arachidonic acid, are located at the *sn*-2 position of glycerol moiety and is released by the action of phospholipase A<sub>2</sub> (PLA<sub>2</sub>) [3]. Arachidonic acid could be metabolized to prostaglandins [4]. In addition, arachidonic acid could undergo lipid peroxidation to generate breakdown products such as 4-hydroxynonenal (HNE) [5]. The latter is a highly reactive aldehyde that impairs the activity of key metabolic enzymes and transporters including sodium, potassium-ATPase, glucose-phosphate dehydrogenase, the glutamate transporter in astrocytes and glucose transporter [6–8]. HNE also impairs the permeability of *in vitro* preparations of the blood-brain-barrier [9]. The levels of HNE are markedly increased in brain and cerebrospinal fluid of patients with neurodegenerative diseases such as Alzheimer disease, Parkinson disease, Huntington disease, and amyotrophic lateral sclerosis [10, 11].

The highest levels of stainable iron in the brain are found in the motor system, with the globus pallidus, substantia nigra pars reticulata, red nucleus and the putamen showing the greatest staining reactivity [12]. Many studies have indicated that iron-induced ROS generation is an important mechanism in producing chronic oxidative stress in neuronal cultures and in brain tissue [13, 14], and a disruption of brain iron homeostasis causing chronic iron accumulation is thought to be associated with oxidative stress in several neurodegenerative dis-

eases and their animal models [15–17]. In contrast, acute neural trauma such as head injury and spinal cord injury may cause sudden increase in iron levels, producing severe oxidative stress in the injured brain. The purpose of our investigation was to study the effect of severe acute oxidative stress on neurons in the hippocampus. This was carried out by a single *in vivo* injection of ferrous ammonium citrate in the rat cerebral ventricle. The model allows us to study the effects of oxidative stress that is free from other factors such as the neuroinflammation, which occur during chronic neurodegeneration [18, 19]. Cellular injury was monitored using immunocytochemistry to HNE, a marker for lipid peroxidation, and cPLA<sub>2</sub>, as well as cell counts in Nissl stained sections, and analyses of Fluro-Jade labeled sections.

## 2. MATERIALS AND METHODS

### 2.1. Animals

Twenty-six male Wistar rats, each weighing approximately 200 g, were purchased from the Laboratory Animals Centre, Singapore. Animals were maintained on a 12 h:12 h light:dark cycle and supplied with standard rat food pellets and water *ad libitum*. All procedures involving animals were in accordance with guidelines of the local Animal Care and Use Committee.

### 2.2. Substances injected

Ferrous ammonium sulphate, citric acid and ammonium citrate (all purchased from Sigma, St. Louis, USA) were all dissolved in sterile distilled water and the pH adjusted to 7.4 with NaOH and HCl, on the day of injection. A concentration of 5 mM ferrous ammonium citrate was freshly prepared prior to each injection, by mixing 1:1 volume of 10 mM ferrous ammonium sulfate and 10 mM citric acid. Ferrous citrate is a potent generator of hydroxyl radicals [20, 21]. A 5 mM concentration of ammonium

citrate was used to control for any additional vehicle effects associated with the ferrous iron solution.

### 2.3. Intracerebroventricular injection and perfusion

Rats were anaesthetized by intraperitoneal injection of 1.2 mL of 7% chloral hydrate, and placed in a stereotaxic head holder with the cranial vault exposed. A 1.0  $\mu$ L of 5 mM ferrous ammonium citrate or ammonium citrate was injected into the anterior horn of the right lateral ventricle (coordinates: 1.0 mm caudal to bregma, 1.5 mm lateral to the midline, 4.5 mm from the surface of the cortex) using a microlitre syringe. The needle was withdrawn 10 min later, and the scalp sutured. Twelve rats were injected with ferrous ammonium citrate, while the remaining fourteen were injected with ammonium citrate as experimental controls. There was no mechanical damage to the hippocampus during the above procedures, since the needle did not contact this tissue. No seizures were observed after the ferrous ammonium citrate or ammonium citrate injection.

The ferrous ammonium citrate injected and ammonium citrate (control) injected rats were sacrificed at 1, 7 and 14 days after injection (4 experimental and 4 control rats at each time interval). They were deeply anaesthetized by intraperitoneal injection of 1.4 mL of 7% chloral hydrate and perfused through the left cardiac ventricle with Ringer's solution followed by a solution of 4% paraformaldehyde in 0.1 M phosphate buffer (pH 7.4). The brains were removed, and post-fixed in the same fixative overnight at 4 °C. Blocks containing the entire rostrocaudal extent of the hippocampus were sectioned coronally at 100  $\mu$ m thickness using a vibrating microtome. The free floating sections were divided into four sets, for immunocytochemical staining for HNE or cPLA<sub>2</sub>, and histochemical staining to detect degenerating neurons using the

cresyl fast violet (Nissl) technique or Fluoro-Jade staining.

### 2.4. Immunocytochemical staining

Sections intended for immunocytochemistry were washed for 3 h in phosphate-buffered saline (PBS, pH 7.4) to remove traces of fixative, and immersed for 1 h in a solution of 2% defatted dry (skimmed) milk in PBS (PBS-milk) to block non-specific binding of antibodies. They were then incubated overnight with monoclonal antibodies to HNE modified proteins (1:200 dilution) or cPLA<sub>2</sub> (Santa Cruz Biotechnology, Santa Cruz, USA, 1:200 dilution). The monoclonal antibody to HNE (HNE Ig4H7) was a kind gift from Dr G. Waeg, and its properties have been described previously [22]. The epitope recognized by this clone is HNE bound to histidine, and this epitope has been recognized on a wide variety of HNE-modified proteins [22]. The antibody to cPLA<sub>2</sub> has been characterized previously, and shown to be specific to cPLA<sub>2</sub> [23]. The sections were then washed in three changes of PBS, and incubated for 1 h at room temperature in a 1:200 dilution of biotinylated horse anti-mouse IgG (Vector, Burlingame, USA). This was followed by three changes of PBS to remove unreacted secondary antibody. The sections were then reacted for 1 h at room temperature with an avidin-biotinylated horseradish peroxidase complex, followed by three changes of PBS. The reaction was visualized by treatment for 5 min in 0.05% 3,3'-diaminobenzidine tetrahydrochloride (DAB) solution in 0.2% nickel-tris buffered saline (N-TBS) containing 0.05% hydrogen peroxide. The color reaction was stopped with several washes of TBS (pH 7.6). Some sections were mounted on gelatin-coated glass slides and lightly counterstained with methyl green before coverslipping with Permount. The remaining sections were processed for electron microscopy. Control sections were incubated with PBS or pre-immune mouse serum instead of primary antibody. These showed absence of immunostaining.

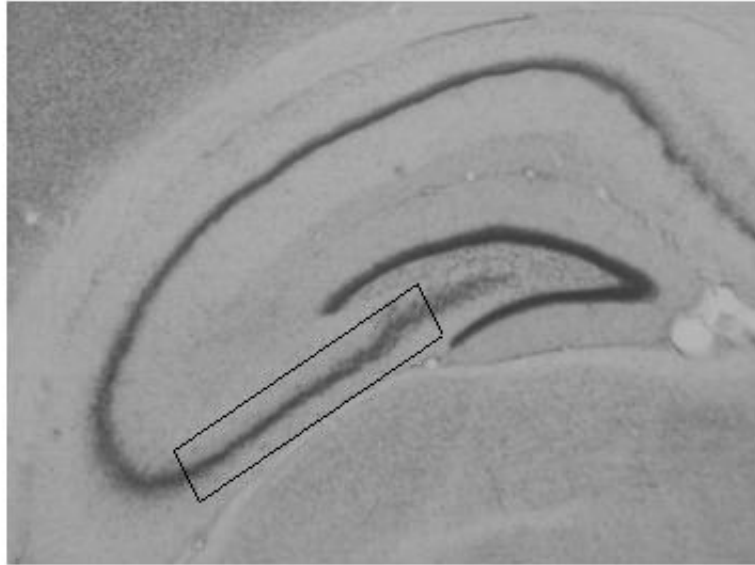


**Figure 1.** Low power light micrograph showing the right hippocampus from a control rat. The boxed area shows the region affected by the ferrous ammonium citrate injections. This area is shown in further detail in Figures 3–6.

### 2.5. Histochemical staining for the detection of degenerating neurons

The third set of sections were mounted on gelatinized slides and stained using the Nissl technique [24]. The fourth set of sections were mounted and stained by the Fluoro-Jade histofluorescent method to detect degenerating neurons [25]. Sections were hydrated in 100% ethanol for 3 min, and 1 min each in 70% ethanol and distilled water, followed by incubation in 0.06% potassium permanganate solution for 15 min, washing in distilled water for 1 min, and incubation in 0.001% Fluoro-Jade solution for 30 min in the dark. The reaction was stopped by three 1 min washes in distilled water. The sections were then cleared in three 2 min changes of xylene, and cover-slipped using Depex water-soluble mountant. The Fluoro-Jade stained sections were examined and imaged with a Carl Zeiss LSM 150 confocal microscope.

### 2.6. Quantification of cells and statistical analysis

These were conducted on the right hippocampus (side of the intracerebroventricular injection) of each rat. A set of three sections each, from the HNE, cPLA<sub>2</sub>, or Nissl stained sections were analyzed. All slides were coded in order to blind the observer to the treatment received by the rats. Images of representative regions, each measuring 255  $\mu\text{m} \times 190 \mu\text{m}$ , of field CA3 of the hippocampus (Fig. 1) were acquired using a Leica Aristoplan microscope fitted with a video camera. The number of stained pyramidal neurons were counted on three each, of the HNE, cPLA<sub>2</sub> or Nissl labeled sections as follows: (1) the sections were taken from the same region of the hippocampus – i.e., the HNE stained sections were adjacent to the cPLA<sub>2</sub> or Nissl stained sections. (2) Only the densely labeled HNE or cPLA<sub>2</sub> labeled pyramidal neurons in the

stratum pyramidale were counted. These neurons were in sharp contrast, and were easily distinguished from, the very lightly labeled pyramidal neurons in the unlesioned portions of the hippocampus [25, 26]. The counts were limited to pyramidal neurons, since preliminary observations showed that these cells had the greatest increases in cell numbers that were densely labeled for HNE and cPLA<sub>2</sub> after ferrous ammonium citrate injection. Although non-pyramidal neurons in the stratum oriens were also labeled, they were far fewer compared to the labeled pyramidal neurons. Likewise, the counts were confined to the right side (side of the intracerebroventricular injection) since the left side showed very few or no labeled cells after injection.

The mean number of stained cells in three sections from each animal was expressed as the number of stained cells/mm<sup>2</sup>. Possible significant differences between the means for the HNE, cPLA<sub>2</sub>, or Nissl stained cells at various post-injection time intervals were analyzed, using 1-way ANOVA with Bonferroni's multiple comparison post-hoc test (SPSS 11.5 for Windows Software.  $P < 0.05$  was considered significant). Possible significant differences between the values of the ferrous ammonium citrate injected and ammonium citrate injected (control) rats were analyzed using the Student's *t*-test ( $P < 0.05$  was considered significant).

### 2.7. Electron microscopy

The remaining HNE or cPLA<sub>2</sub> immunostained sections were subdivided into smaller rectangular portions that included the immunoreactive pyramidal neurons in the CA fields, and processed for electron microscopy using a standard technique [27]. These were osmicated, dehydrated in an ascending series of ethanol and acetone, and embedded in Araldite. Thin sections were obtained from the first 5 μm of the sections, mounted on copper grids coated with Formvar, and stained with lead citrate. They were viewed using a Philips EM1010 electron microscope.

## 3. RESULTS

### 3.1. Light microscopy

#### 3.1.1. HNE immunoreactivity (Figs. 2 and 3)

Control rats injected with ammonium citrate showed  $238.1 \pm 143.7$ ,  $18.2 \pm 16.0$ , and  $31.0 \pm 18.2$  HNE immunostained neurons/mm<sup>2</sup> at 1, 7, and 14 days post-injection, respectively (Fig. 2A). There were only occasional or no HNE labeled neurons in many of the sections (Fig. 3A).

Rats injected with ferrous ammonium citrate showed  $617.8 \pm 159.4$ ,  $454.6 \pm 188.4$ , and  $203.0 \pm 75.3$  HNE immunolabeled neurons/mm<sup>2</sup> at 1, 7, and 14 days post-injection, respectively (Fig. 2A). Dense staining was observed at 1 day post-injection (Fig. 3C). Staining intensity decreased at 7 days (Fig. 3E) and 14 days (Fig. 3F) after injection.

At all three post-injection time intervals, rats injected with ferrous ammonium citrate showed significantly increased number of HNE labeled neurons, compared to rats injected with ammonium citrate ( $P < 0.05$ ).

Rats injected with ferrous ammonium citrate showed significantly decreased number of HNE labeled neurons at 14 days, compared to 1 day post-injection ( $P < 0.05$ ).

#### 3.1.2. cPLA<sub>2</sub> immunoreactivity (Figs. 2 and 4)

Control rats injected with ammonium citrate showed  $295.6 \pm 128.0$ ,  $10.3 \pm 2.9$ , and  $22.8 \pm 13.4$  cPLA<sub>2</sub> immunostained neurons/mm<sup>2</sup> at 1, 7, and 14 days post-injection, respectively (Fig. 2B). There were light or no cPLA<sub>2</sub> labeled neurons in many of the sections (Fig. 4A).

Rats injected with ferrous ammonium citrate showed  $381.8 \pm 163.7$ ,  $571.1 \pm 270.3$ , and  $192.3 \pm 127.1$  cPLA<sub>2</sub> immunostained neurons/mm<sup>2</sup> at 1, 7, and 14 days post-injection, respectively (Fig. 2B). The staining intensity was dense at 1 day (Fig. 4C)

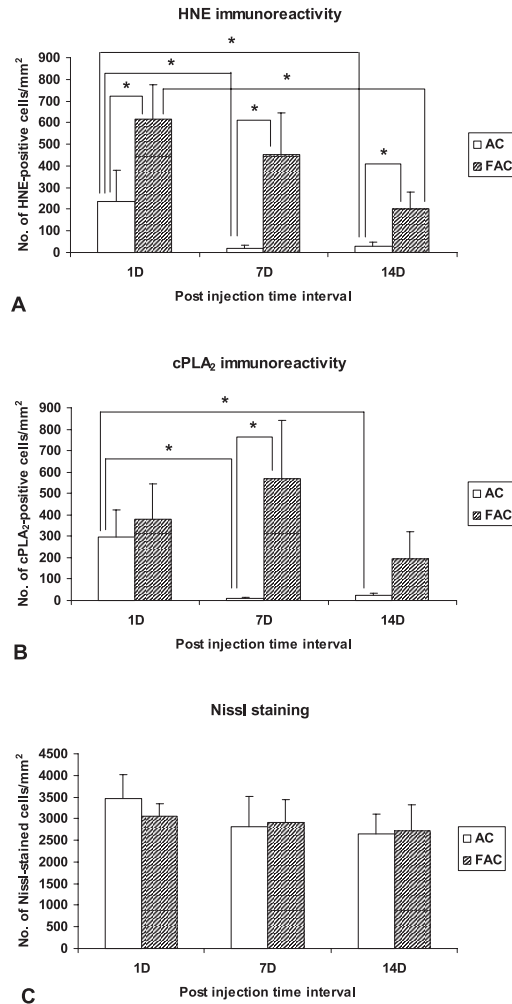


**Figure 2.** Histograms showing the number of HNE, cPLA<sub>2</sub> or Nissl labeled neurons per mm<sup>2</sup> in the stratum pyramidale of the hippocampus. **A:** HNE-immunostained cells. At all three post-injection time intervals, rats injected with ferrous ammonium citrate showed significantly increased number of immunostained cells, compared to rats injected with ammonium citrate. Rats injected with ferrous ammonium citrate showed significantly decreased number of cells at 14 days, compared to 1 day post-injection. Control rats showed significantly decreased number of cells at 7 and 14 days, as compared to 1 day post-injection. **B:** cPLA<sub>2</sub>-immunostained cells. Rats injected with ferrous ammonium citrate showed significantly increased number of cells at 7 days post-injection, compared to rats injected with ammonium citrate. Rats injected with ammonium citrate showed significantly decreased number of cells at 7 and 14 days, compared to 1 day post-injection. **C:** Nissl-stained cells. There were no statistically significant differences between the mean numbers of cells in rats injected with either ammonium citrate or ferrous ammonium citrate at all three post-injection time intervals, indicating no obvious cell death along the row of pyramidal neurons in the CA fields of the hippocampus. Abbreviations: AC, FAC, 1D, 7D, 14D indicate ammonium citrate, ferrous ammonium citrate, 1, 7, and 14 days post-injection. Analyzed by Student's *t*-test, and 1-way ANOVA with Bonferroni's multiple comparison post hoc test. Error bars indicate standard deviation. Asterisks indicate statistically significant differences ( $P < 0.05$ ).

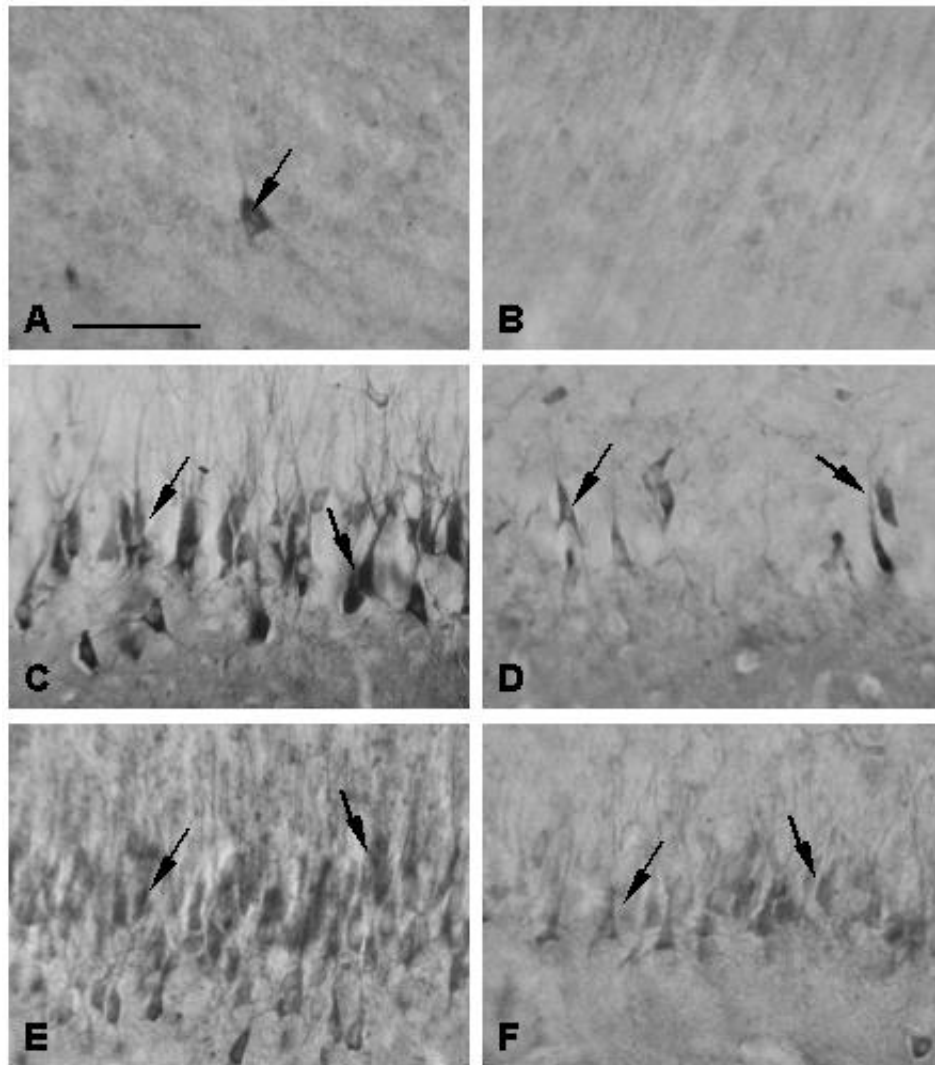


**Figure 3.** Light micrographs of field CA3 of the hippocampus, immunolabeled with a monoclonal antibody to HNE. **A, B:** One week post-ammonium citrate injected rat (control), showing only occasional stained neurons in the stratum pyramidale (arrow) on the side ipsilateral to the intracerebroventricular injection (**A**, right side) and absence of staining on the contralateral side (**B**, left side). **C, D:** One day post-ferrous ammonium citrate injected rat, showing increased number of densely stained pyramidal neurons (arrows) on the ipsilateral side (**C**, right side), and fewer stained neurons (arrows) on the contralateral side (**D**, left side). **E:** The right hippocampus of a 7 day post-ferrous ammonium citrate injected rat, showing dense staining of pyramidal neurons (arrows). **F:** The right hippocampus of a 14 day post-ferrous ammonium citrate injected rat, showing lighter staining of pyramidal neurons (arrows) compared to earlier time intervals. Scale = 50  $\mu$ m.

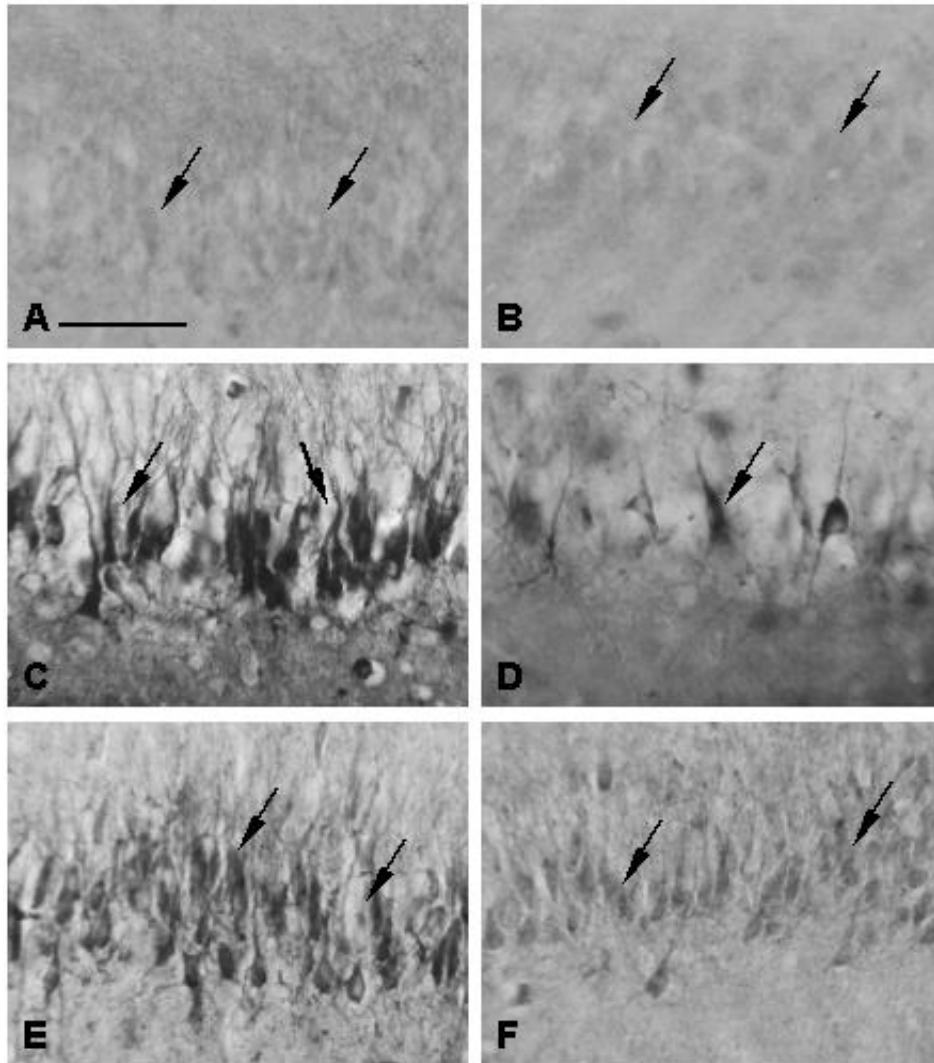


**Figure 4.** Light micrographs of field CA3 of the hippocampus, immunolabeled with a monoclonal antibody to cPLA<sub>2</sub>. **A, B:** One week post-ammonium citrate injected rat (control), showing very little staining in the stratum pyramidale (arrows) on the side ipsilateral to the intracerebroventricular injection (**A**, right side) and absence of staining (arrows) on the contralateral side (**B**, left side). **C, D:** One day post-ferrous ammonium citrate injected rat, showing increased number of densely stained pyramidal neurons (arrows) on the ipsilateral side (**C**, right side), and fewer stained neurons (arrow) on the contralateral side (**D**, left side). **E:** The right hippocampus of a 7 day post-ferrous ammonium citrate injected rat, showing dense staining of pyramidal neurons (arrows). **F:** The right hippocampus of a 14 day post-ferrous ammonium citrate injected rat, showing lighter staining of pyramidal neurons (arrows) compared to earlier time intervals. Scale = 50  $\mu$ m.

and 7 days (Fig. 4E), but light at 14 days (Fig. 4F), after injection.

Rats injected with ferrous ammonium citrate showed significantly increased number of cPLA<sub>2</sub> labeled neurons at 7 days post-injection, compared to rats injected with ammonium citrate ( $P < 0.05$ ).

Rats injected with ammonium citrate showed significantly decreased number of cPLA<sub>2</sub> labeled neurons at 7 and 14 days, compared to 1 day post-injection ( $P < 0.05$ ).

### 3.1.3. Nissl staining and Fluoro-Jade labeling (Figs. 2, 5 and 6)

Control rats injected with ammonium citrate showed  $3475.6 \pm 532.4$ ,  $2825.6 \pm 694.2$ , and  $2635.9 \pm 474.0$  Nissl-stained cell/mm<sup>2</sup> at 1, 7, and 14 days post-injection, respectively (Fig. 2C). The pyramidal neurons in the hippocampus ipsilateral to the intracerebroventricular injections showed similar amounts of Nissl substance, as the neurons on the contralateral side (Figs. 5A and 5B).

Rats injected with ferrous ammonium citrate showed  $3055.2 \pm 299.1$ ,  $2922.9 \pm 513.3$ , and  $2717.2 \pm 600.3$  Nissl-stained cells/mm<sup>2</sup> at 1, 7, and 14 days post-injection, respectively (Fig. 2C). An obvious reduction in Nissl substance was observed in pyramidal neurons at 1 day post-injection (Fig. 5C, 5D), in sections adjacent to those that showed increased HNE or cPLA<sub>2</sub> staining. This, chromatolysis ('loss of color') is due to dispersal, but not loss, of granular endoplasmic reticulum throughout the cell body. The staining of Nissl substance recovered to control levels at 7 days (Fig. 5E) and 14 days post-injection (Fig. 5G).

There were no statistically significant differences between the mean numbers of cells in rats injected with either ammonium citrate or ferrous ammonium citrate at all three post-injection time intervals ( $P > 0.05$ ), indicating no obvious cell death along the row of pyramidal neurons in the CA fields of the hippocampus.

No Fluoro-Jade labeled cells was observed in either the ammonium citrate or ferrous ammonium citrate injected hippocampus at any of the post-injection time intervals, indicating absence of cell loss (Fig. 6).

## 3.2. Electron microscopy (Fig. 7)

### 3.2.1. HNE immunoreactivity

The pyramidal neurons in ammonium citrate injected control rats showed intact cellular and nuclear outlines, intact mitochondria, and absence of large vacuoles in the cytoplasm. Very little or no staining was observed in the cytoplasm (Fig. 7A).

The pyramidal neurons in rats injected with ferrous ammonium citrate contained evenly dispersed, fine heterochromatin (Figs. 7B–7D), in place of the generally clear nucleoplasm in the nucleus of uninjured pyramidal neurons (Fig. 7A). There was also an increase in number of vacuoles in the cell body (Figs. 7B and 7C), and an increase in number of microtubules in the dendrites (not shown). The nuclear and cytoplasmic outlines, and the mitochondria of the labeled cells were however, intact (Figs. 7B–7D). The cells thus had features of injured, but not degenerating neurons. Intense staining was observed at 1 day post-injection (Fig. 7B), but staining intensity decreased at 7 days (Fig. 7C) and 14 days (Fig. 7D) after injection.

### 3.2.2. cPLA<sub>2</sub> immunoreactivity

The neurons that were labeled for cPLA<sub>2</sub> in the ammonium citrate injected or ferrous ammonium citrate injected rats had similar morphological features as those labeled for HNE (Fig. not shown).

## 4. DISCUSSION

The present study aimed to elucidate the possible induction of cPLA<sub>2</sub> and HNE expressions and the effects of such induction on pyramidal neurons of the rat hippocampus, over a period at different time

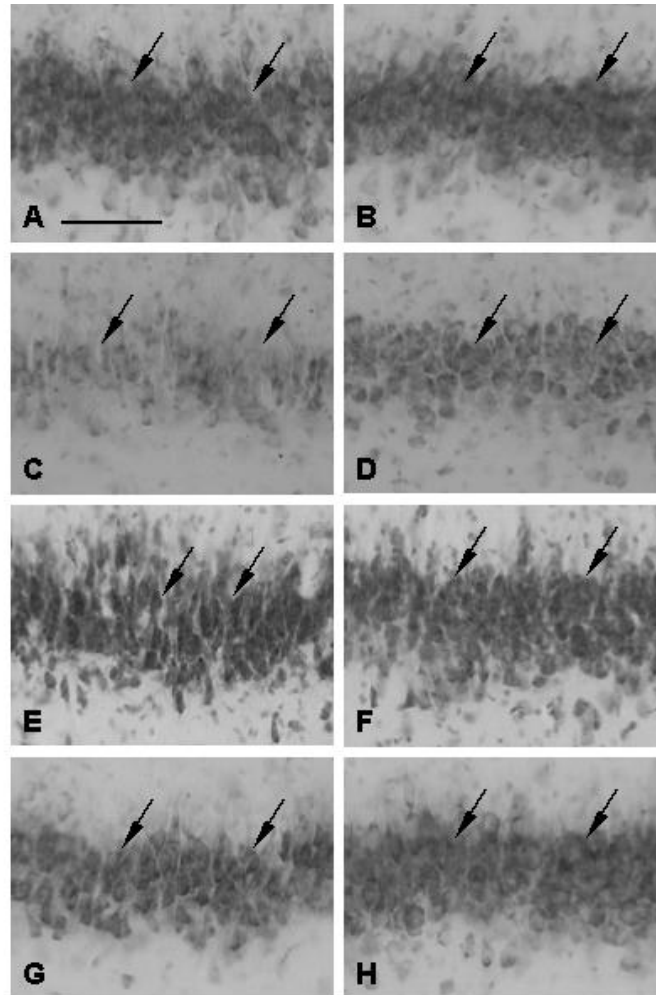


**Figure 5.** Light micrographs of field CA3 of the hippocampus, stained with the Nissl technique. **A, B:** Seven day post-ammonium citrate injected rat (control), showing intact pyramidal neurons (arrows) on the side ipsilateral to the intracerebroventricular injection (**A**, right side) and contralateral side (**B**, left side). Adjacent sections from the same animal are shown in Figures 3A, 3B and 4A, 4B, and 6A. **C, D:** One day post-ferrous ammonium citrate injected rat, showing pyramidal neurons with reduced amounts of Nissl substance (arrows) in the ipsilateral side (**C**, right side) compared to the contralateral side (**D**, left side). This, chromatolysis ('loss of color') is due to dispersal (but not loss) of granular endoplasmic reticulum throughout the cell body. Adjacent sections from the same animal are shown in Figures 3C, 3D and 4C, 4D. **E, F:** Seven day post-ferrous ammonium citrate injected rat, showing intact stratum pyramidale with similar amounts of Nissl substance (arrows) in pyramidal neurons, in both the ipsilateral (**E**) and contralateral (**F**) hippocampus. Adjacent sections of the same animal are shown in Figures 3E, 4E and 6B. **G, H:** Fourteen day post-ferrous ammonium citrate injected rat, showing intact stratum pyramidale with similar amounts of Nissl substance (arrows) in pyramidal neurons, in both the ipsilateral (**G**) and contralateral (**H**) hippocampus. This was despite the injury that had occurred in this area previously, as evidenced by the 'ghost-like' (i.e. very slightly denser) HNE and cPLA<sub>2</sub> immunoreactivity, still visible in the pyramidal neurons in adjacent sections (c.f. Figs. 3F and 4F). Scale = 50  $\mu$ m.

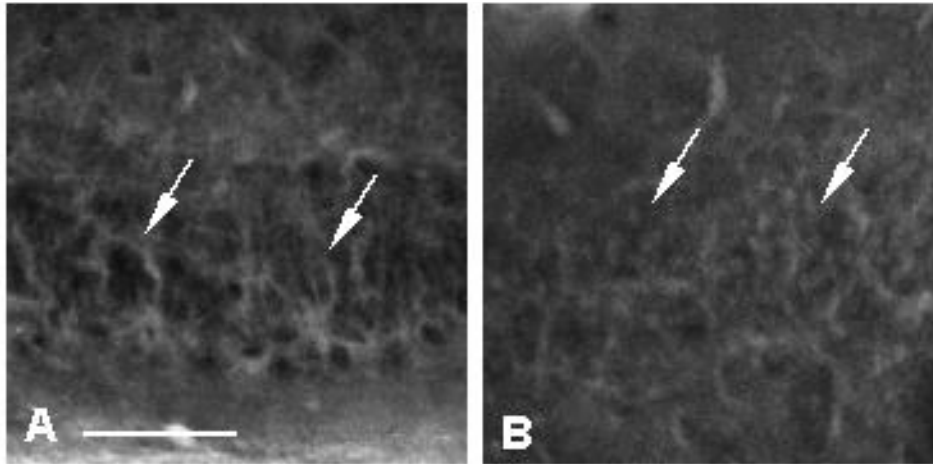


**Figure 6.** Light micrographs of field CA3 of the hippocampus ipsilateral to the injection, stained with Fluoro-Jade. Seven day post-ammonium citrate injected rat (control) (**A**) and (**B**) 1 week post-ferrous ammonium citrate injected rat. Both show absence of any degenerating neurons as evidenced by the lack of Fluoro-Jade labeling. Arrows indicate the stratum pyramidale. Scale = 50  $\mu\text{m}$ .

intervals after a single episode of oxidative stress. An intracerebroventricular injection of 1  $\mu\text{L}$  of 5 mM ferrous ammonium citrate was used to induce severe oxidative stress mediated by hydroxyl radicals. As demonstrated in a previous study, addition of  $\text{Fe}^{2+}$  alone or citrate alone to an *in vitro* cell free system produced little or no  $\cdot\text{OH}$ , whereas addition of  $\text{Fe}^{2+}$  citrate produced a linear increase in  $\cdot\text{OH}$  with time, as detected by the  $\cdot\text{OH}$  adduct of salicylate, 2,3-dihydrobenzoic acid (DHBA). The  $\text{Fe}^{2+}$  citrate complexes closely resemble the intracellular free “labile iron pool” or “transit pool” [28, 29], and these forms were suggested to be present in cases of external iron loading [30]. Therefore this method of inducing oxidative stress may mimic situations where there is increased brain oxidative stress due to iron accumulation *in vivo*.

Ferrous iron, when reacted with an equimolar amount of citric acid, forms tridentate mononuclear complex  $[\text{Fe citrate}]^-$ , which would undergo oxidation and hydrolysis to form tridentate  $[\text{Fe}(\text{OH})\text{citrate}]^-$  and bidentate  $[\text{Fe}(\text{OH})_2\text{citrate}]^{2-}$  ferric complex. During this process,  $\text{Fe}^{2+}$  may be

reduced to form superoxide anion. Furthermore,  $\text{Fe}^{2+}$  itself may take part in an electron transfer reaction with molecular oxygen or with citrate to produce unstable perferryl radicals, forming  $\text{Fe}^{3+}$  and superoxide, leading to the formation of  $\cdot\text{OH}$  by the Haber-Weiss and/or Fenton reaction [28, 29].

An induction of HNE immunoreactivity was observed after ferrous ammonium citrate injection. A significant difference in the number of HNE positive cells was observed between the ferrous ammonium citrate and ammonium citrate injected controls at all time intervals, i.e. 1 day, 1 week and 2 weeks after injection, although the number and density of these labeled cells were significantly fewer in the 2 week post-ferrous ammonium citrate injected rats, than those at 1 day post-injection. Electron microscopy showed that the HNE positive cells had features of injured neurons with evenly dispersed fine heterochromatin in the nucleus, and large numbers of profiles of endoplasmic reticulum, and clear vacuoles in the cytoplasm. The nuclear and cytoplasmic outlines, and the mitochondrial membranes

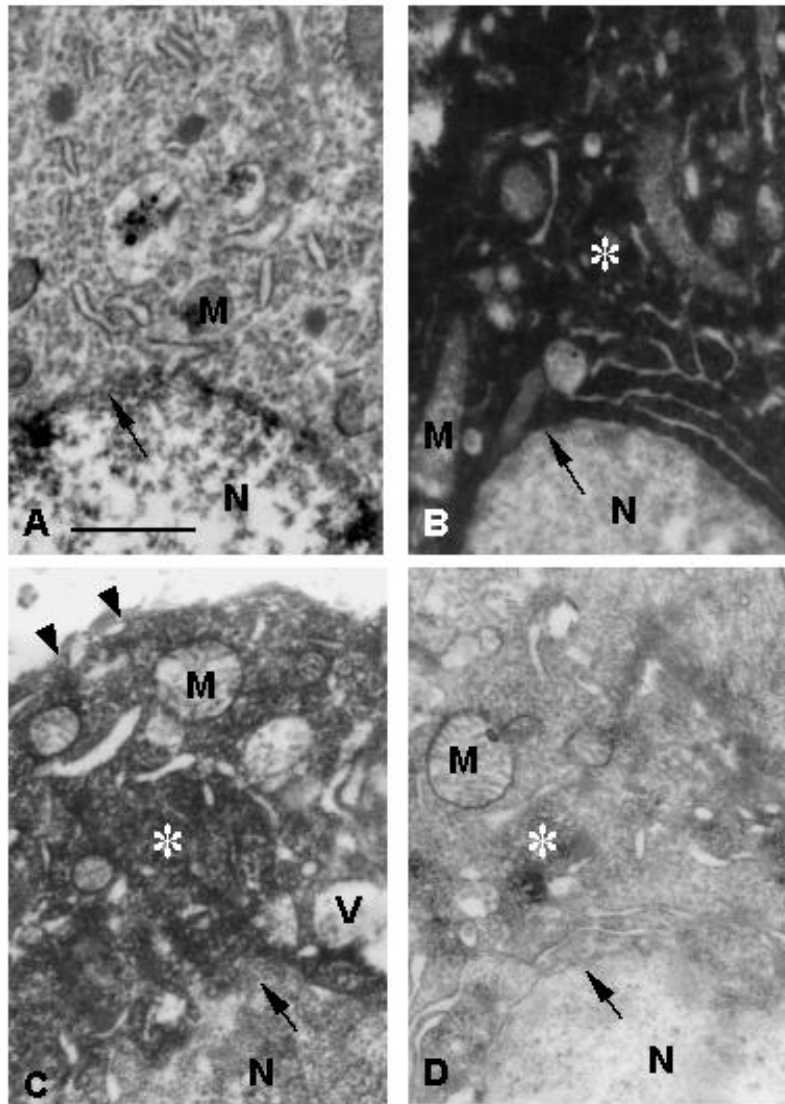


**Figure 7.** Electron micrographs of HNE immunolabeled sections of the hippocampus, from a rat which had been injected with ammonium citrate 7 days previously (**A**, control), and rats which have been injected with ferrous ammonium citrate 1 day (**B**), 7 days (**C**) and 14 days (**D**) previously. **A:** The nucleus of neurons from control rats contained small heterochromatin clumps, and generally light nucleoplasm. Very little or no immunoreaction product is present in the cytoplasm. **B, C, D:** Rats which had been injected with ferrous ammonium citrate showed evenly dispersed fine heterochromatin in the nucleus. There was also an increase in number of vacuoles in the cell body. The nuclear membrane (arrows) and cell membrane (arrowheads), and the mitochondria of the labeled cells are however, intact, and the cells had morphological features of viable cells. Asterisks indicate immunoreaction product. The staining was intense at 1 day post-injection (**B**), but decreased at 7 days (**C**) and 14 days (**D**) after injection. Abbreviations: N: nucleus. M: mitochondrion. V: vacuole. Scale = 1  $\mu$ m.

were, however, intact, and the cells had features of viable neurons. HNE immunoreactivity was observed not only intracellularly, but was also found on the cell membranes. This feature is consistent with the notion that the cell membrane is a major target for hydroxyl radical-induced lipid peroxidation. Such immunoreactivity on the cell membranes was observed in the 1 day and 1 week post-ferrous ammonium citrate injected rats, suggesting that they were cleared by the cells anti-peroxidative mechanism by 1 and 2 weeks post-injection.

An induction of cPLA<sub>2</sub> immunoreactivity was also observed after ferrous ammonium citrate injection. In contrast to HNE staining, however, significant difference between the ferrous ammonium citrate injected and ammonium citrate injected rats was observed only at 1 week post-injection. At 2 weeks post-injection, only faintly labeled cPLA<sub>2</sub> positive cells were observed. cPLA<sub>2</sub> may play a reparative role in removing oxidized fatty acids from the cell membrane after ferrous iron treatment. Phospholipid hydroperoxides are better substrates for cPLA<sub>2</sub> than the native phospholipid [31, 32], and their removal may be essential for the reconstitution of phospholipids with non-peroxidized fatty acid chains. On the other hand, the similar time course and distribution of cPLA<sub>2</sub> and HNE immunoreactivity suggests that cPLA<sub>2</sub> may generate arachidonic acid, which could then be peroxidised to HNE.

A similar induction of cPLA<sub>2</sub> has been observed after exposure of cultured human keratinocytes to UV radiation [33]. Together with the present findings of induction of cPLA<sub>2</sub> expression by ferrous ammonium citrate, they indicate that cPLA<sub>2</sub> could be induced by free radicals. One possibility is that ferrous ammonium citrate-mediated oxidative stress can induce the expression of nuclear factor-kappa B (NF-κB) [34], which is one of the oxidative stress-responsive transcription factors that has been reported to have binding sites on the cPLA<sub>2</sub> promoter, and this binding may induce the

expression of cPLA<sub>2</sub> [35–37]. The transcription factor, *fos* is also increased in times of oxidative stress, and increased *fos* could have bound to the activator protein-1 (AP-1) binding site of cPLA<sub>2</sub> promoter, and induced the expression of cPLA<sub>2</sub> [36].

No seizures were observed in the ferrous ammonium citrate or ammonium citrate injected rats at any of the investigated time point. Although seizures have previously been induced in rats after injection of ferrous chloride, a massive dose was used. The concentration of ferrous ammonium citrate in the ventricles in the present study is estimated at 5 μM (1 μL of a 5 mM solution diluted in approximately 1 mL of cerebrospinal fluid), whereas it has been reported that approximately 3 μL of 100 mM ferrous chloride solution was necessary to induce seizures after injection into the hippocampus [38].

The lack of seizures may account for the difference between the present study and the kainate injection model, in terms of pyramidal cell loss. Although rapid induction of HNE and cPLA<sub>2</sub> were also observed after kainate injection [26, 39], these injections are characterized by the presence of seizures, and hippocampal cell loss obvious in Nissl sections from 3 days post-injection, and a dense glial reaction with many cPLA<sub>2</sub> positive astrocytes in the degenerating hippocampal fields, by 2 weeks post-injection [26]. In contrast, no pyramidal cell loss, or glial reaction (as evidenced by the lack of cPLA<sub>2</sub> positive astrocytes [26, 40]) was observed in this study.

Seizure control was strongly associated with protection against acute lethality and brain pathology, after exposure of guinea pigs to soman and other nerve agents [41]. It is likely that persistent oxidative stress induced by excessive excitotoxic injury induced by glutamate in seizures could have overwhelmed the antioxidant defenses in the neurons, resulting in cell death. In kainate-mediated neuronal death, mitochondrial integrity is lost [26] and HNE concentration is increased to 2.5–4.5 mM

[6, 42], causing rapid cell death associated with depletion of ATP, disturbance in calcium homeostasis, inhibition of key metabolic enzymes and inhibition of protein and DNA synthesis [5].

The damaged neurons were observed to undergo loss of Nissl substance, or chromatolysis at light microscopy. This process has been most studied in motor neurons following axotomy, and involves restructuring of the rough endoplasmic reticulum, accompanied by increased expression of cytoskeletal proteins, but decreased expression of enzymes and receptors related to neurotransmission in the cells. It is thought to reflect efforts of the regenerating neuron to compensate for the injury or lost axon [43]. The cPLA<sub>2</sub> or HNE positive neurons were also observed to have dispersed heterochromatin and increased number of profiles of rough endoplasmic reticulum and mitochondria at electron microscopy. This suggests an increased activity of the cells to generate ATP and synthesize new proteins to counter the effect of the oxidative stress.

The present study therefore shows that in the absence of such repetitive insults, neurons have a remarkable ability to tolerate and recover from a single episode of severe oxidative stress. The concentration of ferrous ammonium citrate injected into the anterior horn of the lateral ventricles (1.0 µL of a 5 mM solution) was sufficient to cause an increase in free radicals [20, 21], but the ability for the neurons to recover from the increased cPLA<sub>2</sub> and HNE immunoreactivity following iron-induced oxidative stress suggests that brain tissue contains endogenous antioxidant mechanisms to protect neurons against neurodegeneration resulting from oxidative injury [44, 45]. Injection of 1 µL of 1 mM ferric ammonium citrate directly into the cerebral cortex resulted in increased expression of the iron binding protein, ferritin in this tissue [14]. Intraneural infusion of iron also resulted in increased activities of the antioxidant enzymes catalase and glutathione peroxidase [13]. These studies indicate that iron binding or free

radical detoxifying systems are increased in brain regions after iron exposure, which reduce the effects of oxidative stress.

Further work is necessary to identify other proteins or lipids that might be induced in recovering neurons after iron induced free radical injury.

#### ACKNOWLEDGEMENTS

This work was supported by a grant from the National University of Singapore (R-223-000-007-112).

#### REFERENCES

- [1] Sayre LM, Smith MA, Perry G. Chemistry and biochemistry of oxidative stress in neurodegenerative disease. *Curr Med Chem* 2001, 8: 721–738.
- [2] Halliwell B, Gutteridge JMC. *Free radicals in biology and medicine*, 3rd ed, Oxford University Press, Oxford and New York, UK, 1999.
- [3] Farooqui AA, Ong WY, Horrocks LA, Farooqui T. Brain cytosolic phospholipase A<sub>2</sub>: Localization, role and involvement in neurological disorders. *Neuroscientist* 2000, 6: 169–180.
- [4] Strokin M, Sergeeva M, Reiser G. Role of Ca<sup>2+</sup>-independent phospholipase A<sub>2</sub> and n-3 polyunsaturated fatty acid docosahexaenoic acid in prostanoid production in brain: perspectives for protection in neuroinflammation. *Int J Dev Neurosci* 2004, 22: 551–557.
- [5] Farooqui AA, Ong WY, Lu XR, Halliwell B, Horrocks LA. Neurochemical consequences of kainate-induced toxicity in brain: involvement of arachidonic acid release and prevention of toxicity by phospholipase A<sub>2</sub> inhibitors. *Brain Res Rev* 2001, 38: 61–78.
- [6] Esterbauer H, Schaur RJ, Zollner H. Chemistry and biochemistry of 4-hydroxynonenal, malonaldehyde and related aldehydes. *Free Radic Biol Med* 1991, 11: 81–128.
- [7] Mark RJ, Lovell MA, Markesbery WR, Uchida K, Mattson MP. A role for 4-hydroxynonenal, an aldehydic product of lipid peroxidation, in disruption of ion homeostasis and neuronal death induced by amyloid β-peptide. *J Neurochem* 1997, 68: 255–264.

- [8] Uchida K. 4-Hydroxy-2-nonenal: a product and mediator of oxidative stress. *Prog Lipid Res* 2003, 42: 318–343.
- [9] Mertsch K, Blasig I, Grune T. 4-Hydroxynonenal impairs the permeability of an in vitro rat blood-brain barrier. *Neurosci Lett* 2001, 314: 135–138.
- [10] Lovell MA, Ehmann WD, Mattson MP, Markesbery WR. Elevated 4-hydroxynonenal in ventricular fluid in Alzheimer's disease. *Neurobiol Aging* 1997, 18: 457–461.
- [11] Zarkovic K. 4-hydroxynonenal and neurodegenerative diseases. *Mol Aspects Med* 2003, 24: 293–303.
- [12] Morris CM, Candy JM, Oakley AE, Bloxham CA, Edwardson JA. Histochemical distribution of non-haem iron in the human brain. *Acta Anat* 1992, 144: 235–257.
- [13] Jacob AK, Hotchkiss RS, Swanson PE, Tinsley KW, Karl IE, Buchman TG. Injection of iron compounds followed by induction of the stress response causes tissue injury and apoptosis. *Shock* 2000, 14: 460–464.
- [14] Bishop GM, Robinson SR. Quantitative analysis of cell death and ferritin expression in response to cortical iron: implications for hypoxia-ischemia and stroke. *Brain Res* 2001, 907: 175–187.
- [15] Connor JR, Menzies SL, St Martin SM, Mufson EJ. A histochemical study of iron, transferrin, and ferritin in Alzheimer's diseased brains. *J Neurosci Res* 1992, 31: 75–83.
- [16] Gutteridge JMC, Halliwell B. Oxidative stress, brain iron and neurodegeneration. In: Olanow CW, Youdim M (Eds.), *Basic principles in Neurodegeneration and Neuroprotection in Parkinson's Disease*, Academic Press, London, 1996, p 1–21.
- [17] Castelnau PA, Garrett RS, Palinski W, Witztum JL, Campbell IL, Powell HC. Abnormal iron deposition associated with lipid peroxidation in transgenic mice expressing interleukin-6 in the brain. *J Neuropathol Exp Neurol* 1998, 57: 268–282.
- [18] Hall ED. Lipid antioxidants in acute central nervous system injury. *Ann Emerg Med* 1993, 22: 1022–1027.
- [19] Wang XS, Ong WY, Connor JR. Increase in ferric and ferrous iron in the rat hippocampus with time after kainate-induced excitotoxic injury. *Exp Brain Res* 2002, 143: 137–148.
- [20] Mohanakumar KP, de Bartolomeis A, Wu RM, Yeh KJ, Sternberger LM, Peng SY, Murphy DL, Chiueh CC. Ferrous-citrate complex and nigral degeneration: evidence for free-radical formation and lipid peroxidation. *Ann N Y Acad Sci* 1994, 738: 392–399.
- [21] Rauhala P, Lin AM, Chiueh CC. Neuroprotection by S-nitrosoglutathione of brain dopamine neurons from oxidative stress. *FASEB J* 1998, 12: 165–173.
- [22] Waeg G, Dimsity G, Esterbauer H. Monoclonal antibodies for detection of 4-hydroxynonenal modified proteins. *Free Radic Res* 1996, 25: 149–159.
- [23] Ong WY, Sandhya TL, Horrocks LA, Farooqui AA. Distribution of cytoplasmic phospholipase A<sub>2</sub> in the normal rat brain. *J Hirnforsch* 1999, 39: 391–400.
- [24] Cox G. Neuropathological techniques. In: Bancroft JD, Stevens A (Eds), *Theory and Practice of Histological Techniques* (2nd ed), Churchill Livingstone, Edinburgh 1982, p 332–363.
- [25] Schmued LC, Albertson C, Slikker W Jr. Fluoro-Jade: a novel fluorochrome for the sensitive and reliable histochemical localization of neuronal degeneration. *Brain Res* 1997, 751: 37–46.
- [26] Sandhya TL, Ong WY, Horrocks LA, Farooqui AA. A light and electron microscopic study of cytoplasmic phospholipase A<sub>2</sub> and cyclooxygenase-2 in the hippocampus after kainate lesions. *Brain Res* 1998, 788: 223–231.
- [27] Hayat MA. *Basic Techniques for Transmission Electron Microscopy*. Academic Press, Orlando, 1986.
- [28] Jacobs A. Low molecular weight intracellular iron transport compounds. *Blood* 1977, 50: 433–439.
- [29] Grootveld M, Bell JD, Halliwell B, Aruoma OI, Bomford A, Sadler PJ. Non-transferrin-bound iron in plasma or serum from patients with idiopathic hemochromatosis. Characterization by high performance liquid chromatography and nuclear magnetic resonance spectroscopy. *J Biol Chem* 1989, 264: 4417–4422.
- [30] Link, G, Pinson A, Hershko C. Heart cells in culture: a model of myocardial iron overload and chelation. *J Lab Clin Med* 1985, 106: 147–153.
- [31] Girotti AW. Lipid hydroperoxide generation, turnover, and effector action in biological systems. *J Lipid Res* 1998, 39: 1529–1542.
- [32] Kambayashi Y, Yamamoto Y, Nakano M. Preferential hydrolysis of oxidized phosphatidylcholine in cholesterol-containing phosphatidylcholine liposome by phospholipase

- A<sub>2</sub>. *Biochem Biophys Res Commun* 1998, 245: 705–708.
- [33] Chen X, Gresham A, Morrison A, Pentland AP. Oxidative stress mediates synthesis of cytosolic phospholipase A<sub>2</sub> after UVB injury. *Biochim Biophys Acta* 1996, 1299: 23–33.
- [34] Schmidt KN, Amstad P, Cerutti P, Baeuerle PA. The roles of hydrogen peroxide and superoxide as messengers in the activation of transcription factor NF- $\kappa$ B. *Chem Biol* 1995, 2: 13–22.
- [35] Morri H, Ozaki M, Watanabe Y. 5'-flanking region surrounding a human cytosolic phospholipase A<sub>2</sub> gene. *Biochem Biophys Res Commun* 1994, 205: 6–11.
- [36] Tay A, Maxwell P, Li Z, Goldberg H, Skorecki K. Isolation of promoter for cytosolic phospholipase A<sub>2</sub> (cPLA<sub>2</sub>). *Biochim Biophys Acta* 1994, 1217: 345–347.
- [37] Anthonsen MW, Andersen S, Solhaug A, Johansen B. Atypical lambda/iota PKC conveys 5-lipoxygenase/leukotriene B<sub>4</sub>-mediated cross-talk between phospholipase A<sub>2</sub>s regulating NF $\kappa$ B activation in response to tumor necrosis factor- $\alpha$  and interleukin-1 $\beta$ . *J Biol Chem* 2001, 276: 35344–35351.
- [38] Willmore LJ, Triggs WJ, Gray JD. The role of iron-induced hippocampal peroxidation in acute epileptogenesis. *Brain Res* 1986, 382: 422–426.
- [39] Ong WY, Lu XR, Hu CY, Halliwell B. Distribution of hydroxynonenal-modified proteins in the kainate-lesioned rat hippocampus: evidence that hydroxynonenal formation precedes neuronal cell death. *Free Radic Biol Med* 2000, 28: 1214–1221.
- [40] Ong WY, Lu XR, Horrocks LA, Farooqui AA, Garey LJ. Induction of astrocytic cytoplasmic phospholipase A<sub>2</sub> and neuronal death after intracerebroventricular carrageenan injection, and neuroprotective effects of quina-crine. *Exp Neurol* 2003, 183: 449–457.
- [41] Shih TM, Duniho SM, McDonough JH. Control of nerve agent-induced seizures is critical for neuroprotection and survival. *Toxicol Appl Pharmacol* 2003, 188: 69–80.
- [42] Bose R, Schnell CL, Pinsky C, Zitko V. Effects of excitotoxins on free radical indices in mouse brain. *Toxicol Lett* 1992, 60: 211–219.
- [43] Kreutzberg GW. Principles of neuronal regeneration. *Acta Neurochir Suppl* 1996, 66: 103–106.
- [44] Delanty N, Dichter MA. Oxidative injury in the nervous system. *Acta Neurol Scand* 1998, 98: 145–153.
- [45] Romero FJ, Bosch-Morell F, Romero MJ, Jareno EJ, Romero B, Marin N, Roma J. Lipid peroxidation products and antioxidants in human disease. *Environ Health Perspect* 1998, 106: 1229–1234.